Atherosclerosis Supplements 40 (2019) 49–54

Contents lists available at ScienceDirect

Atherosclerosis Supplements

journal homepage: www.elsevier.com/locate/atherosclerosis

Optical coherence tomography of retinal and choroidal layers in patients with familial hypercholesterolaemia treated with lipoprotein apheresis

Claudia Stefanutti [a], Dario Mesce [a], Fernanda Pacella [b], Serafina Di Giacomo [a], Paolo Turchetti [c], Michele Forastiere [b], Edoardo Trovato Battagliola [b], Giuseppe La Torre [d], Gianpaolo Smaldone [b], Elena Pacella [b, *]

[a] Extracorporeal Therapeutic Techniques Unit, Lipid Clinic and Atherosclerosis Prevention Centre Regional Centre for Rare Diseases, Immunohematology and Transfusion Medicine, 'Umberto I' Hospital, Department of Molecular Medicine, Sapienza University of Rome, Italy
[b] Department of Sense Organs, Faculty of Medicine and Dentistry, Sapienza University of Rome, Italy
[c] National Institute for Health, Migration and Poverty (INMP/NIHMP), Rome, Italy
[d] Department of Public Health and Infectious Diseases, Faculty of Pharmacy and Medicine, Sapienza University of Rome, Italy

Keywords:
Optical coherence tomography
OCT
Optic coherence tomography-angiography
OCT-Angiography
OCTA
Familial hypercholesterolaemia
Retinal vascular alterations

A B S T R A C T

Purpose: Detect and quantify morpho-functional alterations of the retina and choroid in patients affected by familial hypercholesterolemia (FH) treated with lipoprotein apheresis (LA) using optic coherence tomography (OCT) and optic coherence tomography-angriography (OCTA).
Design: Observational study.
Subjects: To be diagnosed: A group of 20 patients (40 eyes) being clinically and genetically diagnosed as FH and under treatment (FH-Group)", for at least 2 years, was compared to a control group of 20 healthy subjects (40 eyes), with a normal lipid profile and no ocular disease (CT-Group).
Methods: Participants were studied with the slit lamp, binocular indirect fundoscopy, OCT and OCTA.
Main outcome measures: Best corrected visual acuity (BVCA), spherical equivalent (SE), intraocular pressure (IOP), central macular thickness (CMT), choroidal thickness (CHT), retinal nerve fiber layer in four quadrants (RNFL (Superior = Sup; Inferior = Inf; Nasal = Nas Temporal = Temp), and the mean value across the four quadrants (RNFL G), foveal avascular zone (FAZ) and vascular density (VD).
Results: FH subjects had smaller RNFL superiorly ($108 \pm 19{,}38$ μm OD/$111 \pm 16{,}56$ μm OS FH-Group vs $127 \pm 7{,}42$ μm OD/$129 \pm 14{,}64$ μm OS CT-Group; $P < 0{,}001$ for both OD and OS) and inferiorly ($108 \pm 23{,}58$ μm OD/$115 \pm 17{,}33$ μm OS FH-Group vs $128 \pm 18{,}15$ μm OD/$133 \pm 17{,}38$ μm OS CT-Group; $P = 0{,}002$ OD; $P = 0{,}001$ OS). G RNFL was consequently smaller ($93 \pm 12{,}94$ μm OD/$94 \pm 10{,}49$ μm OS FH-Group vs $101 \pm 9{,}01$ μm OD/$101 \pm 10{,}20$ μm OS CT-Group; $P = 0{,}03$ OD; $P = 0{,}02$ OS). FH subjects had a larger FAZ ($0{,}31 \pm 0{,}08$ mm^2 OD/$0{,}33 \pm 0{,}10$ mm^2 in OS FH-Group vs $0{,}21 \pm 0{,}05$ mm^2 OD/$0{,}21 \pm 0{,}07$ mm^2 OS CT-Group; $P < 0{,}001$ OD; $P = 0{,}002$ OS).
Conclusions: Early signs of retinal vessel damage in FH patients can be detected and quantified with OCT and OCTA.

1. Introduction

Familial hypercholesterolaemia (FH) is defined as a group of genetic diseases characterized by very high levels of circulating low-density lipoproteins (LDL). Heterozygous FH (HeFH) is one of the most common congenital metabolic diseases in the western population, affecting 1 every 300/500 persons [1–3]. Based on this data, it can be inferred that about 10 millions people are affected worldwide. FH is caused by a mutation in the genes coding for the low-density lipoprotein receptor (LDLR), its ligand Apolipoprotein B (ApoB-100), or the proprotein convertase subtilisin/kexin type 9 (PCSK9), which is an essential enzyme for LDLR degradation [4–6].

* Corresponding author. Umberto I Hospital, Viale del Policlinico 155 - Cap 00161, Rome, Italy.
E-mail address: elena.pacella@uniroma1.it (E. Pacella).

https://doi.org/10.1016/j.atherosclerosissup.2019.08.031
1567-5688/

Abbreviations

OD	right eye
OS	left eye
SE	spherical equivalent
BVCA	best corrected visual acuity
IOP	intraocular pressure
CMT	central macular thickness
CHT	choroidal thickness
FAZ	foveal avascular zone
RNFL	retinal nerve fiber layer
VD	vascular density
FH	familial hypercholesterolaemia
LDL	low-density lipoproteins
LDLR	low-density lipoprotein receptor
ApoB-100	ligand apolipoprotein B
PCSK9	proprotein convertase subtilisin/kexin type 9
CHD	coronary vessel disease
OCT	optic coherence tomography
OCTA	OCT-angiography
EDI	enhanced-depth imaging
ETDRS	early treatment diabetic retinopathy study
LA	lipoprotein apheresis

Main clinical manifestations are due to the accumulation of cholesterol esters in peripheral tissues and include: tendon xanthomas, cutaneous xanthelasma in limb extremities, periocular tissue and corneal arch. The very high levels of LDL-C cholesterol and total cholesterol in FH patients induce over time premature coronary vessel disease (CHD), leading to angina pectoris and myocardial infarction [7]. Males and females affected by FH, aged between 20 and 39 years, present a 100-fold risk of developing premature CHD compared to the rest of the population [8]. FH-induced atherosclerosis mostly involves coronary vessels, but also affects carotid arteries, abdominal aorta and lower limb vessels, including femoral, popliteal and tibial arteries. These patients are also at risk for stroke and abdominal aortic aneurysm [9].

Retinal arterial vessels are not exempt from atherosclerotic involvement, even in subjects without hypercholesterolemia. Microvascular alterations in this area strongly correlate to the development and prognosis of both cardiac and cerebrovascular pathologies. The AIRC study demonstrated that a decrease in lumen size of retinal vessels is associated to an increased risk for stroke, mostly of ischemic type [10]. This correlation has also been confirmed in the Cardiovascular Health Study [11].

Recently, optic coherence tomography (OCT) has acquired an increasingly central role in the diagnosis and management of multiple retinal pathologies [12]. OCT-angiography (OCTA) allows for the acquisition of high-resolution images of the intraretinal circulation, the quantification of macular edema and to highlight a highly reflective embolic plaque inside the optic nerve head [13,14]. Currently there are not many studies on the change of choroid or retina in untreated heterozygotes or in homozygous FH. In this study, we explored whether OCT and OCTA were able to detect and quantify – either directly or indirectly – retinal vessel atherosclerosis in patients affected by FH.

2. Materials and methods

This is a retrospective study of consecutive FH patients under care at the 1) Extracorporeal Therapeutic Techniques Unit, Lipid Clinic and Atherosclerosis Prevention Centre, Immunohematology and Transfusion Medicine, Department of Molecular Medicine; 2) Department of Sense Organs, Faculty of Medicine and Dentistry, "Umberto I" Hospital, Sapienza University of Rome, Italy. A written informed consent was obtained from each patient.

The study included two groups of patients. One group (FH-Group) included 20 patients (40 eyes) affected by FH. Their demographic and clinical features are reported on Table 1. These patients were diagnosed and treated in the Lipid Clinic of our hospital. The second group served as control (CT-Group) and included 20 healthy subjects (40 eyes), randomly selected from a pool of patients refferred to our Eye Emergency Unit. Their demographic and clinical features are reported on Table 2.

Table 1
Demographic and clinical features of FH subjects included in the study.

ID	Gender	Age	Treatment	Years of LA*
1	F	36	Drug therapy and LA*	18
2	F	67	Drug therapy and LA*	16
3	F	37	Drug therapy and LA*	22
4	F	64	Drug therapy and LA*	5
5	M	70	Drug therapy and LA*	7
6	F	66	Drug therapy and LA*	6
7	M	38	Drug therapy and LA*	13
8	M	60	Drug therapy and LA*	4
9	F	32	Drug therapy and LA*	4
10	M	33	Drug therapy and LA*	5
11	F	40	Drug therapy and LA*	15
12	F	64	Drug therapy and LA*	23
13	M	37	Drug therapy and LA*	9
14	F	58	Drug therapy and LA*	9
15	F	32	Drug therapy and LA*	17
16	M	42	Drug therapy and LA*	11
17	M	61	Drug therapy and LA*	6
18	M	41	Drug therapy and LA*	5
19	F	60	Drug therapy and LA*	20
20	F	63	Drug therapy and LA*	17

* LA: lipoprotein apheresis.

Table 2
Demographic and clinical features of subjects without familial hypercholesterolemia serving as controls.

ID	Gender	Age	Treatment	Years of LA*
1	F	39	None	N/A
2	F	68	None	N/A
3	M	33	None	N/A
4	F	63	None	N/A
5	M	70	None	N/A
6	F	40	None	N/A
7	M	61	None	N/A
8	M	58	None	N/A
9	F	57	None	N/A
10	F	36	None	N/A
11	F	36	None	N/A
12	M	40	None	N/A
13	M	33	None	N/A
14	F	59	None	N/A
15	F	58	None	N/A
16	M	60	None	N/A
17	F	43	None	N/A
18	M	61	None	N/A
19	F	36	None	N/A
20	M	41	None	N/A

* LA: lipoprotein apheresis.

3. Inclusion criteria

1. FH phenotipic and genetic diagnosis lasting at least two years;
2. Treatment with drug therapy and lipoprotein apheresis;
3. Spherical equivalent (SE) between −3 and +3 diopters;

4. Exclusion criteria

1. Congenital or acquired pathologies associated to significant retinal or choroidal damage;
2. Prescription of topical therapy for a chronic eye condition;
3. History of eye surgery in the last 6 months.

Each participant underwent the following investigations:

- Visual acuity (expressed in LogMAR);
- Biomicroscopic examination at the slit lamp;
- Photograph of the posterior segment and binocular indirect fundoscopy;
- Goldmann applanation tonometry;
- Retinography, OCT and OCTA: to study the retina and choroid;

5. Autorefractor and best-corrected visual acuity

The autorefractor adopted is Tomey RC-800 Auto Ref/Ker, used in both static and dynamic refraction modes. Refractive error is expressed in spherical equivalent. Visual acuity in each patient was assessed with the charts of the Early Treatment Diabetic Retinopathy Study (ETDRS), at a distance of 4 m. Patients were invited to identify letters on each row. Best corrected visual acuity (BVCA) was measured using the total number of correctly identified letters and the LogMAR score of the row in which patient identified three or more letters with the best possible visual correction.

6. Slit lamp biomicroscopy and tonometry

Ocular physical exam was conducted using the slit lamp Haag Streit 900 B, which also allowed image acquisition. FH-GROUP patients were evaluated accurately for the principal ocular and periocular lesions associated to FH (corneal arch and palpebral xanthelasma), as well as other possible tissue alterations presumptively associated to FH and not present in the CT-GROUP. Ocular pressure was measured with Goldmann applanation tonometer after anesthetizing the corneal surface with Benoxinate 0.4% eye drops.

7. Posterior segment biomicroscopy and indirect binocular fundoscopy

The posterior segment was visualized at the slit lamp using a 90D lens. We searched for morphological alterations at the macula or posterior pole. Some of the expected alterations included: changes in caliber or branching pattern of the retinal vascular tree (angiosclerosis, arterovenous crossing), morphological and structural macular changes (macular dystrophy/atrophy, pigmentary changes), cholesterol emboli, peripapillary atrophy. Binocular indirect fundoscopy was performed with OMEGA500 ophthalmoscope and a 20D lens. We searched for alterations in middle or extreme retinal periphery in FH-GROUP subjects.

8. Retinography

Fundus was photographed using Fundus Camera Topcon TRC-50DX. Measurement of retino-choroidal thickness and morphology was performed with Spectralis HRA-OCT software, by Heidelberg Engineering (version 3.2), using the following settings: 512 x 49-scan volume scanning (49 lines, 512 A-scan for each line); 6 × 6 mm scanning area; image acquisition time of 15 s; 6-mm radial scans, 30° intervals, centered at the fovea. Enhanced-depth imaging algorithm was used to improve visualization of the choroid. Average central macular thickness (CMT), measured in microns (μm), was extrapolated from the map reconstructed after volumetric scanning; choroidal thickness (CHT), measured in microns (μm), was measured after segmenting retino-choroidal layers. CHT was measured manually, after drawing a perpendicular line to the retinal layer, from Bruch's membrane to the sclerochoroidal junction, at the center of the fovea. For this purpose, we used the image with the highest resolution of the sclerochoroidal junction.

We quantified retinal nerve fiber layer (RNFL) thickness using RNFL scanning protocol (image diameter of 3,4 mm, centered at the papilla). RNFL thickness was the mean of all the recorded values using the *fast RNFL thickness protocol* (3 scans for each of the 256 measurement points; image acquisition took 1.8 s). Thickness of each quadrant (Sup, Inf, Nas, Tem) and the mean of the four values (G = Global) was computed. The foveal avascular zone (FAZ) was measured manually from OCTA images and was expressed in mm [2]. OCTA images were obtained with Angio-OCT OPTUVE using the following settings: 3 × 3 mm area; 5 B-scan reiterations of 500 A-scans; 500 raster positions; center on the fovea. The whole process took 3.9 s. In addition, Vasal Density (VD%) was calculated in the same area using Vessel Density ILM-RPE algorithm; both superficial and deep retinal plexi were included in this mathematical analysis.

Table 3
Clinical and morpho-structural characteristics of FH-Group subjects.

Number of patients (eyes)	20 (40)	
Age (Mean ± SD)	50,05 ± 13,68 years	
Gender (M/F)	8/12	
Eye	OD	OS
SE* D (Mean ± SD)	0,01 ± 1,478	0,12 ± 1,655
BCVA† Letters (Mean ± SD)	57 ± 9.60	58,35 ± 2,83
IOP mmHg‡ (Mean ± SD)	14.9 ± 1,45	15 ± 1,59
CMT** μm (Mean ± SD)	251,5 ± 21,55	255 ± 19,17
CHT†† μm (Mean ± SD)	389,8 ± 70,85	392,3 ± 60,13
FAZ‡‡ mm^2 (Mean ± SD)	0,31 ± 0,08	0,33 ± 0,10
RNFL*** Sup. μm (Mean ± SD)	108 ± 19,38	111 ± 16,56
RNFL*** Inf. μm (Mean ± SD)	108 ± 23,58	115 ± 17,33
RNFL*** Tem.μm (Mean ± SD)	75 ± 12,81	71 ± 12,67
RNFL*** Nas. μm (Mean ± SD)	76 ± 11,05	77 ± 11,11
RNFL***G μm (Mean ± SD)	93 ± 12,94	94 ± 10,49
VD††† % (Mean ± SD)	43,69 ± 3,28	44,88 ± 4,04
Corneal arch	15% (3)	
Xantelasma	10% (2)	
Cholesterol emboli	5% (1)	
Retinal Vascular Alterations	50% (10)	
Macular Alterations	20% (4)	
Peripapillary Atrophy	10% (2)	

This table presents the ocular characteristics of a group of 20 patients (40 eyes) affected by familial hypercholesterolemia for at least 2 years (FH-Group).
* SE: spherical equivalent.
† BVCA: best corrected visual acuity.
‡ IOP: intraocular pressure.
** CMT: central macular thickness.
†† CHT: choroidal thickness.
‡‡ FAZ: foveal avascular zone.
*** RNFL: peripapillary retinal nerve fiber layer.
††† VD: vascular density.

Table 4
Clinical and morpho-structural characteristics of CT-Group subjects.

Number of patients (eyes)	20 (40 eyes)	
Age (Mean ± SD)	49,60 ± 12,46	
Gender (M/F)	9/11	
Eye	OD	OS
SE* D (Mean ± SD)	0,33 ± 1,20	0,33 ± 1,32
BCVA† Letters (Mean ± SD)	59 ± 1,45	58,35 ± 3,34
IOP‡ mmHg (Mean ± SD)	14,6 ± 1,46	15,3 ± 1,22
CMT** μm (Mean ± SD)	258,2 ± 14,06	256,6 ± 15,04
CHT†† μm (Mean ± SD)	408,4 ± 89,81	395,85 ± 7,42
FAZ‡‡ mm^2 (Mean ± SD)	0,21 ± 0,05	0,21 ± 0,07
RNFL*** Sup. μm (Mean ± SD)	127 ± 7,42	129 ± 14,64
RNFL*** Inf. μm (Mean ± SD)	128 ± 18,15	133 ± 17,38
RNFL*** Tem.μm (Mean ± SD)	75 ± 9,19	66 ± 8,14
RNFL*** Nas. μm (Mean ± SD)	74 ± 13,86	75 ± 11,45
RNFL***G μm (Mean ± SD)	101 ± 9,01	101 ± 10,20
VD††† % (Mean ± SD)	45,20 ± 4,16	44,48 ± 3,28
Cholesterol Emboli	0% (0)	
Retinal Vascular Alterations	20% (4)	
Macular Alterations	10% (2)	
Peripapillary Atrophy	10% (2)	

This table presents the ocular characteristics of a group of 20 healthy subjects (40 eyes) serving as control (CT-Group).
* SE: spherical equivalent.
† BVCA: best corrected visual acuity.
‡ IOP: intraocular pressure.
** CMT: central macular thickness.
†† CHT: choroidal thickness.
‡‡ FAZ: foveal avascular zone.
*** RNFL: peripapillary retinal nerve fiber layer.
††† VD: vascular density.

8.1. Statistical analysis

All parameters are expressed in the following format: mean ± SD. ANOVA and Fisher tests were used to compare the two groups. Results were regarded statistically significant if $p < 0.05$ (5%).

9. Results

Summary of morpho-structural characteristics of FH-Group and CT-Group subjects are presented in Tables 3 and 4 respectively.

As shown in Table 5, groups were compared on the following parameters: BCVA, SE, IOP, CMT, CHT, RNFL (Sup, Inf, Nas, Temp, G), FAZ, and VD%. FH subjects had a smaller RNFL in two quadrants: superior (108 ± 19,38 μm OD/111 ± 16,56 μm OS FH-GROUP vs 127 ± 7,42 μm OD/129 ± 14,64 μm OS CT-GROUP; P < 0,001 OD; P < 0,001 OS) and inferior (108 ± 23,58 μm OD/115 ± 17,33 μm OS FH-GROUP vs 128 ± 18,15 μm OD/133 ± 17,38 μm OS CT-GROUP; P = 0,002 OD; P = 0,001 OS). As depicted on Fig. 1, RNFL global value (RNFL G or Tot) was consequently smaller (93 ± 12,94 μm OD/94 ± 10,49 μm OS FH-GROUP vs 101 ± 9,01 μm OD/101 ± 10,20 μm OS CT-GROUP; P = 0,03 OD; P = 0,02 OS). As shown on Fig. 2, FH patients also displayed a larger FAZ (0,31 ± 0,08 mm2 OD/0,33 ± 0,10 mm2 in OS FH-GROUP vs 0,21 ± 0,05 mm2 OD/0,21 ± 0,07 mm2 OS CT-GROUP; P < 0,001 OD; P = 0,002 OS).

Furthermore, 50% of FH-Group subjects presented with retinal vascular alterations on fundoscopy, which is in contrast to 20% in the CT-Group.

10. Discussion

In our study, we used OCT and OCTA to study the retina and choroid of patients affected by FH. We compared these subjects to their controls on the following parameters: BCVA, SE, IOP, CMT, CHT, RNFL (Sup, Inf, Nas, Temp, G), FAZ, and VD%. Our goal was to identify which parameters differed between the two groups and use them as early indicators of retinal microvascular atherosclerosis. We noted statistically significant differences in RNFL Sup., RNFL Inf., RNFL G, and FAZ.

For what concerns RNFL, our results are in accordance with those of the Beijing Eye Study [15] (China, 2006), which enrolled 3251 adult patients affected by dyslipidemia. The purpose was to identify ocular alterations more prevalent in this population. Differences in visual acuity and refractive error were not statistically significant. However, patients with dyslipidemia were found to have a higher IOP mean and suffered more from peripapillary atrophy, even if that was not associated to glaucomatous damage. Similarly – in our study – we found a generalized reduction in RNFL thickness, especially in the superior and inferior quadrants, where fibers are more numerous. However, mean IOP did not differ

Table 5
Comparison between FH-Group and CT-Group.

Parameter	*Mean ± SD FH-Group*		*Mean ± SD CT-Group*		*Mean Difference*		*P-value*	
Eye	OD	OS	OD	OS	OD	OS	OD	OS
SE* (D)	0,01 ± 1,478	0,12 ± 1,655	0,33 ± 1,20	0,33 ± 1,32	0,22	0,21	0,42	0,63
BCVA† (letters)	57 ± 9.60	58,35 ± 2,83	59 ± 1,45	58,35 ± 3,34	2,00	0,00	0,42	0,38
IOP‡ (mmHg)	14.9 ± 1,45	15 ± 1,59	14,6 ± 1,46	15,3 ± 1,22	−0,30	0,30	0,50	0,51
CMT** (μm)	251,5 ± 21,55	255 ± 19,17	258,2 ± 14,06	256,6 ± 15,04	−18,60	3,60	0,26	0,77
CHT†† (μm)	389,8 ± 70,85	392,3 ± 60,13	408,4 ± 89,81	395,85 ± 7,42	6,70	1,60	0,45	0,85
FAZ‡‡ (mm^2)	93 ± 12,94	94 ± 10,49	101 ± 9,01	101 ± 10,20	−0,10	−0,11	<0,001	0,002
RNFL*** Sup. (μm)	0,31 ± 0,08	0,33 ± 0,10	0,21 ± 0,05	0,21 ± 0,07	20,65	18,00	<0,001	<0,001
RNFL*** Inf. (μm)	108 ± 19,38	111 ± 16,56	127 ± 7,42	129 ± 14,64	21,80	17,80	0,002	0,001
RNFL*** Temp. (μm)	108 ± 23,58	115 ± 17,33	128 ± 18,15	133 ± 17,38	−0,50	−5,00	0,88	0,14
RNFL*** Nas. (μm)	75 ± 12,81	71 ± 12,67	75 ± 9,19	66 ± 8,14	−3,30	−1,45	0,45	0,66
RNFL***G (μm)	76 ± 11,05	77 ± 11,11	74 ± 13,86	75 ± 11,45	7,90	7,45	0,03	0,02
VD††† %	43,69 ± 3,28	44,88 ± 4,04	45,20 ± 4,16	44,48 ± 3,28	1,33	0,40	0,26	0,73

This table presents compares the ocular characteristics of patients affected by familial hypercholesterolemia (FH-Group) with their controls (CT-Group).
* SE: spherical equivalent.
† BVCA: best corrected visual acuity.
‡ IOP: intraocular pressure.
** CMT: central macular thickness.
†† CHT: choroidal thickness.
‡‡ FAZ: foveal avascular zone.
*** RNFL: peripapillary retinal nerve fiber layer. Sup: superior. Inf: inferior. Tem: temporal. Nas; nasal. G: global value, mean of the four values.
††† VD: vascular density.

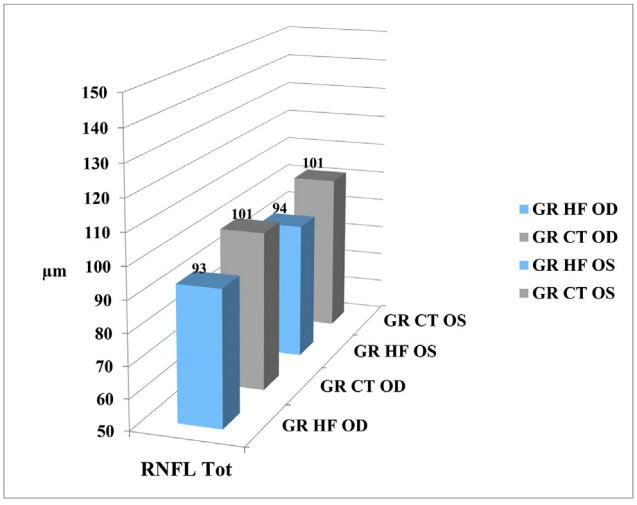

Fig. 1. Comparison of RNFL G (RNFL Tot) for OD and OS between the familial hypercholesterolemia group (GR HF) and the control group (GR CT).

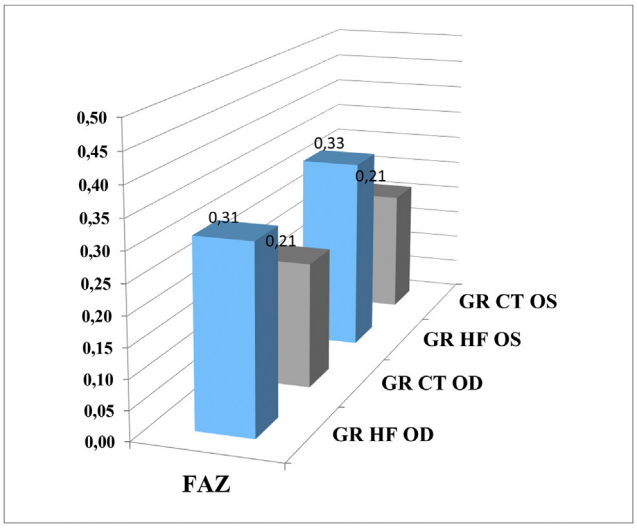

Fig. 2. Comparison of FAZ for OD and OS between the familial hypercholesterolemia group (GR HF) and the control group (GR CT).

from that of the control group. Further research is encouraged to describe the pathophysiological process linking high cholesterol levels and axonal damage in retinal ganglion cells.

Regarding FAZ, the mean value of this parameter was higher in FH patients compared to their controls. Additionally, the presence of angiosclerosis on fundoscopy was a more common occurrence in these same patients. Our results are similar to those published by Kim et al. [16], which enrolled patients affected by diabetic retinopathy. In these patients, the mean FAZ value was 0,21 mm^2 higher than that of healthy controls. Diabetic retinopathy, cigarette smoking, hypertension, inflammation and alcohol consumption – similarly to FH – is characterized by retinal vessel damage of occlusive-ischemic type and associated to an elevated CV risk [17]. Rarefaction of foveal capillaries and consequent enlargement of the foveal avascular zone could be the result of a chronic ischemic condition affecting retinal vessels, determined by the generalized atherosclerotic process occurring in FH patients. Of note – in our study –, VD% did not correlate to the FAZ. This apparent inconsistency could be explained by the relatively recent introduction of OCTA [16], which may not be sophisticated enough to accurately segment the superficial and deep capillary plexi.

In conclusion, the choroidal and vascular alterations of retinal foveal capillaries in FH patients can be studied and quantified with OCT and OCTA. In particular, the FH-Group when compared to the CT-Group, showed an enlargement of FAZ probably secondary to chronic atherosclerotic ischemic process. Moreover, through the use of OCT and OCTA imaging, in addition to staging the degree of the disease, it is also possible to evaluate the efficacy of treatment during its course and on long-term follow-up [18,19]. Similar vascular abnormalities of retinal foveal capillaries have also been observed in subjects with hypertension, state of inflammation, alcohol consumers and cigarette smokers [20].

However, further research on a larger sample size is desirable before the aforementioned parameters can be used as early indicators of retinal microvascular atherosclerosis.

Financial support

None.

Declaration of competing interest

The authors have no conflict of interest to declare in relation to the preparation and submission of this article.

No proprietary interest exists for any author.

Acknowledgements

This article is part of a supplement entitled 'Therapeutic Apheresis – Current advances for the treatment of metabolic, cardiovascular and autoimmune diseases. Based on the contributions to the 2nd Congress of the European Group – International Society for Apheresis, March 22-24, 2018, Vienna, Austria', published with support of the European Group – International Society for Apheresis – E-ISFA office. E-ISFA gratefully acknowledges support of this supplement by B. Braun, DIAMED Medizintechnik, Fresenius Medical Care, and Kaneka.

References

[1] Goldstein JL, Schrott HG, Hazzard WR, Bierman EL, Motulsky AG. Hyperlipidemia in coronary heart disease. II. Genetic analysis of lipid levels in 176 families and delineation of a new inherited disorder, combined hyperlipidemia. J. Clin. Investig. 1973;52(7):1544–68.
[2] Scriver Charles R. The metabolic and molecular bases of inherited disease. McGraw-Hill; 2001. p. 2863–913.
[3] Moriarty PM. LDL-apheresis therapy. Curr. Treat. Options Cardiovasc. Med. 2006;8(4):282–8.
[4] Innerarity TL, Mahley RW, Weisgraber KH, et al. Familial defective apolipoprotein B-100: a mutation of apolipoprotein B that causes hypercholesterolemia. J. Lipid Res. 1990;31(8):1337–49.
[5] Abifadel M, Varret M, Rabès JP, et al. Mutations in PCSK9 cause autosomal dominant hypercholesterolemia. Nat. Genet. 2003;34(2):154–6.
[6] Sjouke B, Hovingh GK, Kastelein JJ, Stefanutti C. Homozygous autosomal dominant hypercholesterolaemia: prevalence, diagnosis, and current and future treatment perspectives. Curr. Opin. Lipidol. 2015;26(3):200–9.
[7] Hobbs HH, Brown MS, Goldstein JL. Molecular genetics of the LDL receptor gene in familial hypercholesterolemia. Hum. Mutat. 1992;1(6):445–66.
[8] Civeira F, Jarauta E, Cenarro A, et al. Frequency of low-density lipoprotein receptor gene mutations in patients with a clinical diagnosis of familial combined hyperlipidemia in a clinical setting. J Am. Coll. Cardiol. 2008;52(19):1546–53.
[9] Owen CG, Rudnicka AR, Nightingale CM, et al. Retinal arteriolar tortuosity and cardiovascular risk factors in a multi-ethnic population study of 10-year-old children; the Child Heart and Health Study in England (CHASE). Arterioscler. Thromb. Vasc. Biol. 2011;31(8):1933–8.
[10] Wong TY, Klein R, Couper DJ, et al. Retinal microvascular abnormalities and incident stroke: the atherosclerosis risk in communities study. Lancet 2001;358(9288):1134–40.
[11] Longstreth W, Larsen EK, Klein R, et al. Associations between findings on cranial magnetic resonance imaging and retinal photography in the elderly:

the Cardiovascular Health Study. Am. J. Epidemiol. 2007;165(1):78–84.
[12] Schneider M, Müller HP, Lauda F, et al. Retinal single-layer analysis in Parkinsonian syndromes: an optical coherence tomography study. J. Neural. Transm. (Vienna) 2014;121(1):41–7.
[13] Jia Y, Bailey ST, Wilson DJ, et al. Quantitative optical coherence tomography angiography of choroidal neovascularization in age-related macular degeneration. Ophthalmology 2014;121(7):1435–44.
[14] Quaranta-el maftouhi M, El maftouhi A, Eandi CM. Chronic central serous chorioretinopathy imaged by optical coherence tomographic angiography. Am. J. Ophthalmol. 2015;160(3):581–587.e1.
[15] Wang S, Xu L, Jonas JB, You QS, Wang YX, Yang H. Dyslipidemia and eye diseases in the adult Chinese population: the Beijing eye study. PLoS One 2012;7(3):e26871.
[16] Kim DY, Fingler J, Zawadzki RJ, et al. Noninvasive imaging of the foveal avascular zone with high-speed, phase-variance optical coherence tomography. Investig. Ophthalmol. Vis. Sci. 2012;53(1):85–92.
[17] La Torre G, Pacella E, Saulle R, et al. The synergistic effect of exposure to alcohol, tobacco smoke and other risk factors for age-related macular degeneration. Eur. J. Epidemiol. 2013;28(5):445–6. May.
[18] Pacella E, La Torre G, Impallara D, et al. Efficacy and safety of the intravitreal treatment of diabetic macular edema with pegaptanib: a 12-month follow-up. Clin. Ter. 2013;164(2):e121–6.
[19] Stefanutti C, Julius U, Watts GF, et al. Toward an international consensus-Integrating lipoprotein apheresis and new lipid-lowering drugs. MIGHTY MEDIC Multinational Society. J. Clin. Lipidol. 2017;11(4):858–71.
[20] Takayama K, Kaneko H, Ito Y, et al. Novel classification of early-stage systemic hypertensive changes in human retina based on OCTA measurement of choriocapillaris. Sci. Rep. 2018;8(1):15163.